Applications of diffusion weighted imaging in detection of radiating pain to lower extremities

Reza Mohammadi[1], Fariborz Faeghi[2*], Ayoob Rostamzadeh[3], Jalal Jalal Shokouhi[4], Doman Arefan[5]

1. Department of Radiology Technology, Faculty of Paramedicine, Shahid Beheshti University of Medical Sciences, Tehran, Iran.
2. Department of Radiology Technology, Faculty of Allied Medical Sciences, Shahid Beheshti University of Medical Sciences, Tehran, Iran.
3. Department of Anatomical Sciences, Faculty of Medicine, Shahrekord University of Medical Sciences, Shahrekord, Iran.
4. Iranian Society of Radiology, Central committee, Tehran, Iran.
5. Department of Medical Radiation, Shahid Beheshti University of Medical Sciences, Tehran, Iran.

Corresponding author: Tel: +98 9127171638 Fax: +98 2122711131
Address: Department of Radiology Technology, Faculty of Allied Medical Sciences, Ghods Square, Tehran, Iran.
E-mail: f_faeghi@sbmu.ac.ir
Received; 2015/04/5 revised; 2015/05/25 accepted; 2015/06/7

Abstract

Introduction: To examine the hypothesis that diffusion weighted imaging (DWI) in lumbosacral region could reveal sciatic nerve course swelling that lead to lower extremity pain. The aim of present article was to find and evaluate the diffusion weighted coefficients (b-values) for scrutinizing sciatic nerve tract changes in lumbosacral region.

Materials and methods: Lumbar area was imaged in 30 patients with lower extremity pain in one side (left or right) at 1.5 T MR with routine protocols and DWI. Two stages for processing images were generated. Distance of sciatic nerve fibers between all patients In terms of Gray level average (GLA) and Contrast average (CA) on each side were calculated by MATLAB software. An appropriate statistical test such as Paired T test was used and. $P<0.05$ was considered as significant

Results: In the first stage of image processing there was no significant result in affected side rather than normal side. In the second stage, the mean b-value was significantly correlated with affected side that represent nerve swelling and the mean ADC was positively related to affected side. In b-value images, the diameter of affected side is greater than the healthy side and $P<0.001$ showed significant results. The CA of affected side is greater than healthy side and $P<0.001$ illustrated significant results. For GLA, statistics showed the greater values for affected side in comparison to healthy side and $P<0.001$ was significant.

Conclusion: Based on the results of present study, neurography is possible way to visualize early changes, such as nerve indentation and swelling, and to qualitatively evaluate affected lumbar nerves course in patients with lower extremity pains.

Keywords: Diffusion weighted imaging, Lumbar spine, Neurography, ADC Map, Claudicating

Introduction

For the first time, the radicular pain of sciatica was explained by Mixter and Barr (1) but the underlying pathophysiology remains unknown. Disk compression is a frequent event that occurs among people and related to many things such as

heredity, age, the history of occupations, driving, sitting history and any other things (2). Low back pain is now recognized as the most common and expensive ailment of the middle-aged patients in the industrialized societies of western nations (3). In parallel to disk compression results on nerve roots, sometimes without any direct nerve involvement a rupture in disk or annular tear could result radiating pain to lower extremity (4, 5), this finding represent the possibility of patients complain about low back pain despite having normal MRI imaging of Lumbosacral region. Among patients with low back pain and unilateral or bilateral radiation to lower extremities, the pain arises from within the disk. In these cases, pain radiating to lower limb seems to be a referred type and seems unrelated to direct nerve root compression or irritation by disk fragment in the epidural space (6). The disk herniation caused widespread edema throughout the entire nerve root using CT myelograms (7). Gadolinium–DTPA-enhanced MRI showed enhancement of symptomatic nerve roots among patients with Lumbar-herniated disks and the degree of enhancement reflected the severity of the sciatica (8). If the patient problems arise from nerve root and disk disease we can diagnose by doing routine MRI that it will be done in most medical imaging centers (9, 10). Patients with lumbosacral and lower extremity pain may be referred to clinics with normal reported routine Lumbosacral MRI but they do have radiating pain to the lower extremities. Unilateral lower limb extremity pain is more often happen than two sided pain. T2W spin-echo conventional techniques cannot image smaller nerves in periphery because the nerves cannot be distinguished from blood vessels on T2W spin-echo images (11). Diffusion weighted imaging (DWI) can reveal microstructure of tissues on the basis of giving information about random movement of water molecules, which is restricted in some directions due to tissue

damages (12). Moreover, the net displacement of molecules is called apparent diffusion coefficient (ADC) and a sequence can be sensitized to this motion by applying two gradients on either side of the 180o radiofrequency (RF) pulse (9, 10). This works in the similar way to phase contrast Magnetic Resonance Angiography (MRA) in that stationary spins will acquire no net phase change after the gradients have been applied. Moving spins, however, will acquire this phase change and result in signal loss (9). In diffusion imaging, normal tissue has lower signal intensity than abnormal tissue, the molecules within are free to move, while diffusion becomes restricted when pathology is present. The signal change depends on ADC of tissue and the strength of the gradients. The amplitude of these is controlled by the b factor/value which is similar to VENC (Encoding Velocity) in phase contrast MRA (10, 12). Recently, it has been reported that DWI is useful for assessment and diagnosis of lesions, such as those patients who suffer from multiple sclerosis (13) and peripheral nerve compression disorders, such as carpal tunnel syndrome (14). However, imaging of spinal cord, disks and vertebra with DWI have technical limitations. The small size of cord and susceptibility artifacts which related to tissue/bone interfaces make problem in DWI imaging of the Lumbosacral region (15). To test hypothesis that diffusion weighted imaging in lumbosacral region could reveal sciatic nerve course swelling, lead to lower extremity pain. Thus we decided to apply optimized version of DWI sequences to collect more details about patient problems. The aim of this article was to find and evaluate the diffusion weighted coefficients (b-values) for scrutinizing sciatic nerve tract changes in lumbosacral region.

Materials and methods

Study population: Thirty patients (16 males and 14 females; median age: 42.7

years; range: 18-69 years) participated in our study, with radiating pain to lower extremities mainly and solely in one side, after being examined with routine lumbosacral MRI, they were examined by DWI. Thus the other side values were used as control population. Testimonial was obtained from all patients before the study and study was approved by the Beheshti University of Medical Sciences research Committee. Inclusion criteria was to determine patients who had one side claudicating and the exclusion criteria were; a) having surgery history in lumbar area or hip; b) Trauma in this region; c) Having bilateral symptoms and two sided

radiculopathy and d) Lumbar canal stenosis. The duration of lower extremity pain before MRI was determined 8-10 weeks.

MRI protocol: We used a 1.5 T scanner (I Class, B17 software, Avanto, Siemens Medical System; Germany). Subjects were examined in supine position and they were studied in routine lumbosacral MRI examinations by using Torso array coils. DWI was performed in coronal plane by using a short TI inversion recovery–echo planar imaging (STIR–EPI) sequence (multishot echo planar (EPI imaging) with free breathing technique. Table 1 illustrates image parameters in our study.

Table 1. The parameters for imaging of patients.

Parameters	Sequence					
	TR (ms)	TE (ms)	TI (ms)	Slice thickness (mm)	Distance factor (mm)	Number of slices
DWI	5000	89	180	3	0	22
	b-value s/mm^2	Field of view (mm)	Matrix size	Acceleration factor	EPI factor	Total scan time
	50/300/500/700	352×352	192×192	2	96	2 min 36 seconds

Image analysis: With this DWI sequence we acquired tissues image with an impeded diffusion, for instance spinal cord, nerve roots and peripheral nerves. The use of a short TI inversion recovery for fat suppression ensured elimination of disturbing signals as we had in fat, blood vessels, tendons and muscles, although the acquired images by using this technique were low in signal to noise ratio because of using fat suppression. After acquiring DWI images the

b-value 300 s/mm2 series were transferred to Maximum Intensity Projection software of system (MIP). Images with 5 mm thicknesses in favorite orientation (coronal) were constructed for better nerve tracking. With coronal reconstruction in MIP software the trajectory of main nerves was acceptably visualized. Using 4 b-values help us to obtain more precise ADC map results. In Figure 1 we can observe the images with 4 b-values reconstructed in coronal plane.
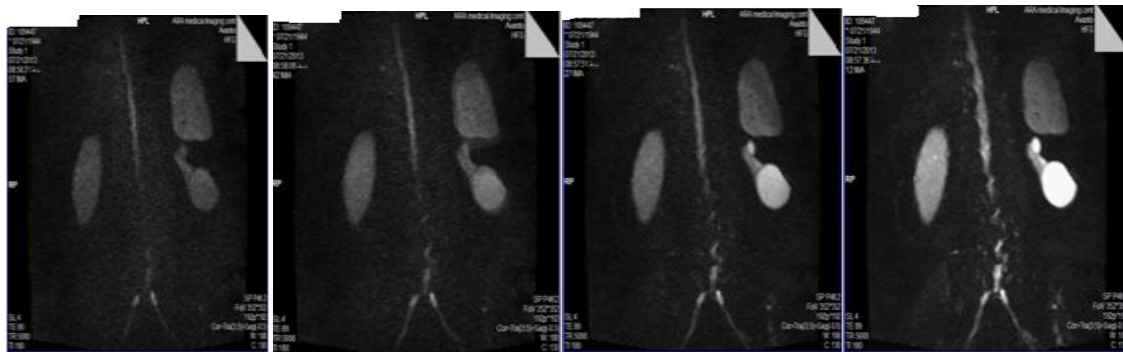
Figure 1. Reconstructed images with 5 mm slice thicknesses in coronal plane (right to left) with b-values 50/300/500/700 s/mm^2. As we can see the plane of reconstructed images was set in coronal plane. The coronal reconstructions were set in planes, that we have the complete length of nerves branching down from the lower end of the spinal cord.

3

Two stages of image processing were done on result of images. In first stage of research three regions of interest (ROIs) in b-values include: 300 s/mm2 images with 21 pixels extends put on each side (healthy side and affected side) on the nerve and the same story for corresponding apparent diffusion coefficient (ADC maps) images. The values are taken for more comparison (Figure 2). On the other hand, we performed second stage of research, a program in MATLAB software generated to cut unwanted parts of images and focus on main objects for processing images without artifacts.
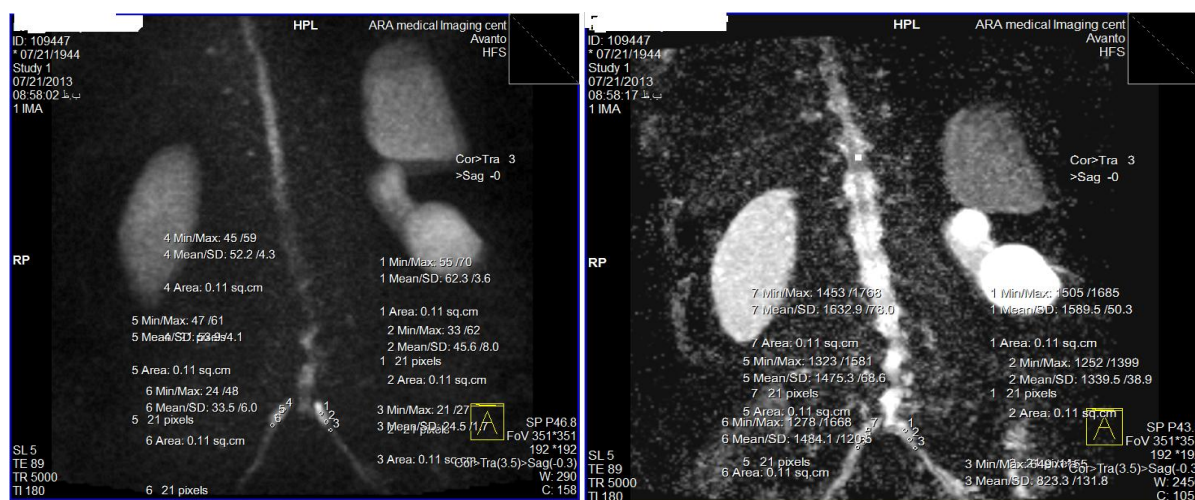
Figure 2. The images above show the b-value 300 (left) and the ADC map (right) of 39 old year's patient. We chose 3 ROIs with 21 pixels extend on each side of each image. These values represent the amount of signal/noise ratio on each ROI.

We first input the reconstructed image in MIP to software and splitting it to right and left side with similar dimensions (length and width) for equally and separately process. We use smoothing filter after previous session for eliminating unwanted noises, then Binary conversion with Wiener method would change the image format to binary system. Then we use dilation method on binary resulted image and input the result image for region growing labeling. The last result would be the binary image only contains the main object and we can extract the features of image such as mean diameter, mean contrast and mean density of each sciatic nerve fiber of each side. Figure 3 shows the processing order in MATLAB software. We used this program to calculate details in similar distance of sciatic nerve fibers between all patients for :

1) Mean nerve diameter on each side.
2) Gray level average (GLA) on each side.
3) Contrast average (CA) on each side

Statistical analysis

Statistical analysis was performed by SPSS software (Version 20). In this study we focus on L5-S1 trunk (nerve). Paired T test was used to compare the extracted values. $P<0.05$ was considered significant.
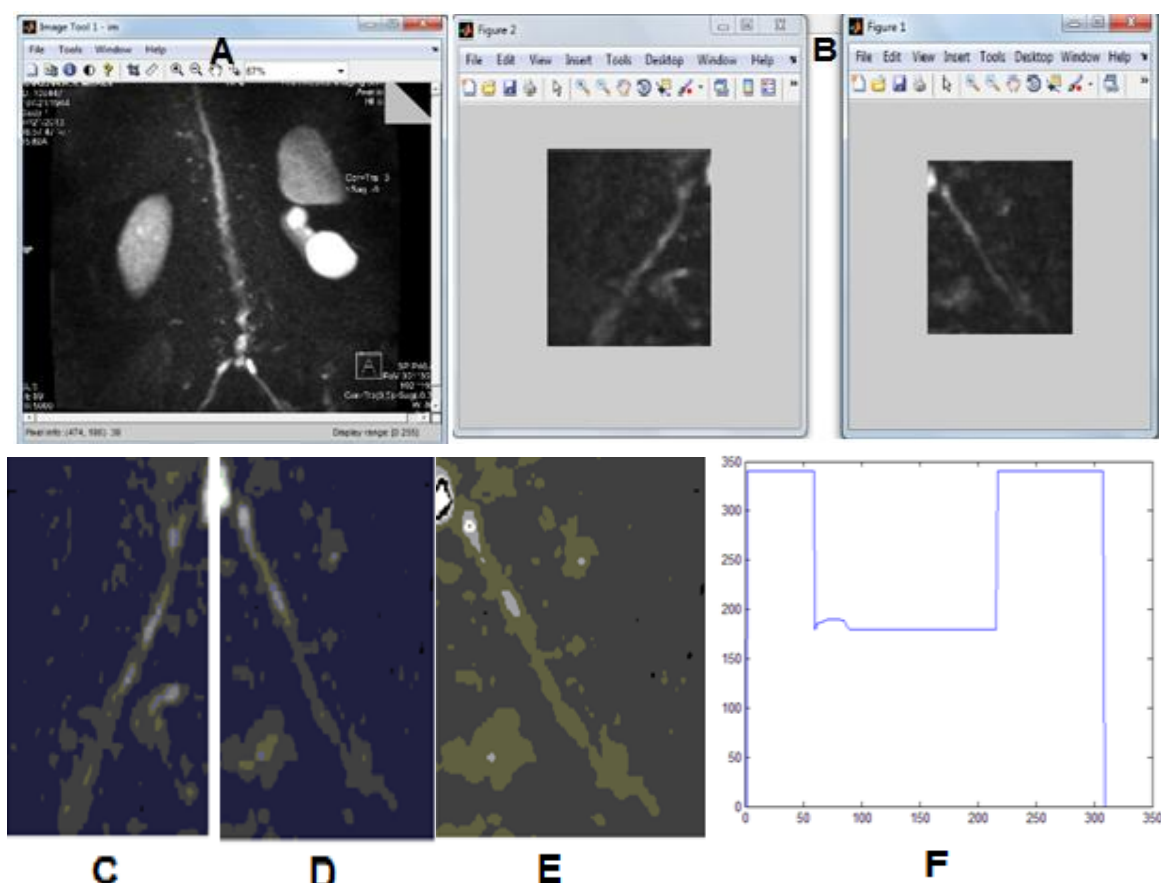
Figure 3. Different levels of image processing in MATLAB software. A) Illustrates the image selection and finding a start point. B) Illustrates the image division. C, D) Noise elimination and smoothing. E) Otsu matrix module and Binary conversion. F) The chart of changing nerve diameter on one side in selected length.

Results

We used Paired t-test to compare data we acquired from right and left sides (affected side versus healthy side). Statistics extracted from image survey, so, first stage shows the mean selected ROIs on ADC map on affected side was 1167.51 and on healthy side was 1135.16. It means that affected side is a bit higher than healthy side. In comparison to healthy side the ADC shows insignificant results (P=0.305). The mean selected ROIs on b-value 300 on affected side were 40.85 and on healthy side were 38.51. The story was the same as ADC values for this parameter. Again affected side shows values a bit higher than healthy side but it is not significant in meaning (P=0.159). We expected the b-values of affected side higher than healthy side and ADC values of affected side lower than healthy side. Table 2 summarizes statistics we collected in first stage of research.

Table 2. Summarize the Healthy and Affected sides in first stage.

Patients	Healthy side mean (SD)	Affected side mean (SD)	Difference mean (SD)	%95 CI	P-value†
b-value= 300	38.51	40.85	2.34	(-0.96 , 5.66)	0.159
ADC	1135.16	1167.51	32.34	(-30.98 , 95.67)	0.305

†In b-value images, the P= 0.159 which is a positive value greater than 0.05 and it means no statistically significant results. In ADC images, the P= 0.305 which is a positive value greater than 0.05 and it means no statistically significant importance.

Statistics extracted from image survey, in second stage: we had three parameters for comparison including:

1. The mean diameter of nerve tract in b-value 300 images on affected side was 52248.83; this is greater than healthy side 51442.86. These numbers for ADC of affected side was 54999.23 and for healthy side 53955.40. We expect having greater b-values in affected side than healthy side and the opposite for ADC values. The statistics show significant results in both parameters (P<0.001) but the results in ADC was not clinically acceptable. Actually the ADC had to be with lower values in affected side (Tables 3 and 4).

2. The GLA on affected side in b-value 300 was 223.03 and on healthy side was 221 and these numbers for ADC of affected side was 234.30 and for healthy side was 230.63. In both ADC and b-value images P- value were less than 0.001. It means that there are significant results in ADC and b-value. For b-value images, the statistics could be accepted based on hypothesis of this study. We anticipated the ADC values in affected side to be less than healthy side due to ADC and b-value image characteristics, but the ADC showed significant statistics in negative way and we couldn't accept the results (Tables 3 and 4).

3. The mean CA in b-value 300 images on affected side was 248.86 and on healthy side were 248.33. These numbers for ADC images of affected side was 244.36 and the healthy side was 242.50. Again statistics showed significant results in both ADC and b-value, but results that obtained in ADC images were not clinically acceptable due to opposite character of ADC with b-value. Tables 3 and 4 show the statistics we collected from second stage of image processing.

Table 3. Summarize the b-value 300 parameters between healthy and affected sides in second stage.

Patients	Healthy side mean (SD)	Affected side mean (SD)	Difference mean (SD)	P-value
Diameter	51442.86	52248.83	805.97	< 0.001
GLA‡	223.03	221	2.03	< 0.001
CA†	248/33	248/86	0.53	< 0.001

‡Gray level average, †Contrast average.

Table 4. Summarize the ADC parameters between healthy and affected sides in second stage.

Patients	Healthy side mean (SD)	Affected side mean (SD)	Difference mean (SD)	%95 CI	P-value
Diameter	53955.40	54999.23	1043.83	(788.92 , 1298.74)	< 0.001
GLA‡	230. 63	234.30	3.66	(2.51 , 4.82)	< 0.001
CA†	242.50	244.36	1.86	(1.35 , 2.38)	< 0.001

‡Gray level average, †Contrast average.

In b-value images, the diameter of affected side is greater than healthy side and P<0.001 showed significant results. The CA of affected side is greater than healthy side and P<0.001 showed significant results. For GLA statistics illustrated differences between affected side and healthy side, the mean difference between this two sides showed the P<0.001 that means significant results. In ADC images, the diameter of affected side is greater than healthy side and the P<0.001 that showed significant results. The CA of affected side is greater than healthy side and the P<0.001 showed significant results. For GLA statistics show greater values for affected side in comparison to healthy side and P<0.001 was significant. In b-value parameters we obtained expected results in affected side, although the ADC maps show significant results but we expected lower numbers in ADC of affected side than normal side. The statistics we obtained in ADC were unacceptable despite its p-value. All we were chasing described greater b-value in affected side

rather than normal side and lower ADC value in affected side rather than normal side. May be we have to examine and process the findings among greater population.

Discussion

The power of DWI imaging in case of specificity and sensitivity in evaluating early changes in many diseases such as MS, Stroke, Trauma, Tumors and Infection (16) has become as an essential part of armamentarium of routine diagnostic sequences in MRI. The increasingly diagnostic potentials of DWI pop create an idea in our minds to work on lumbosacral region. DWI may be useful to provide information which is not available with conventional MR imaging in evaluating of spine, disks, spinal cord and nerves. The power of DWI to detecting early and microstructure changes may help us to diagnose disease affected sciatic nerve (11). Many studies have done on DWI and ADC on degeneration discs and spinal cord. A statistically significant decrease was seen in ADC values of degenerated lumbar disks when it compared to ADC values of normal disks. More caudal disks, even when they are normal, showed lower ADC values than more cephalic disks (17). On the other hand, we know that the lumbar intervertebral disks are the largest vascular tissue in adult human body. Thus, its nutrition occurs by means of diffusion from blood vessels in the surrounding structures (18). Maybe changes in blood vessels supply can affect herniation of disk cause widespread edema throughout the entire nerve root and can be find in myelograms. It means that myelography could clearly illustrate swelling in affected nerve root (19). Several authors have described that in gadolinium-DTPA-enhanced MRI the symptomatic nerve roots in patients affected by lumbar-herniated disks would show enhancement. The degree of enhancement reflected the severity of sciatica (8, 20). In 2011 using

DWI in study by Beattie PF and his colleagues reveal that DWI sequence might allow the differentiation of potentially quantify the physiologic effect of physical therapy intervention in normal and degenerative lumbar intervertebral discs (21). In present study, mean ADC values in affected side of patient were greater than in healthy side. Also the b-value 300 showed greater values in affected side than in healthy side. In this study we used STIR-EPI sequences and free breathing scanning technique, and then we provided 3D reconstructed images for tracking the course of nerve in MIP images. We generally focused on L5-S1 nerve that exiting down of pelvic that's branching to thigh. According to the nerve distribution dermatome (22) we focused on L5-S1 tract in this study but chasing the nerve course can be done in other to study for remaining nerve tracts. The results of first stage assessment in this study showed that the mean ADC and b-value 300 in affected side are often greater than healthy side except in a few number of patients (may be the difference referring to the cause of disease, the time period of disease or other parameters) (17, 21). Anyway, in first stage we could not reach to reliable results in this study. In second stage the statistics of patients showed the greater ADC and b-values in affected side than in healthy side of the patient. We expected the b-values of affected side would be greater than healthy side. Statistics show coordinate results, but the mean ADC in the affected side tended to increase and it is against what we expected (it had to be decreased) (11). In the second parameter of the second stage, CA, b-value parameters in affected side were meaningful and greater than healthy side (P<0.05), and it's the same for ADC map images. In the last parameter of second stage, the GLA, this parameter in both b-values and ADC map in affected side were greater than healthy side and for mean ADC maps the story was the same, it means despite our expectation it increased

7

(13, 17, 21). In result, we think greater population of patients could eliminate any doubt (if exist) and lead to increase of statistical power. We acknowledge that present study has several conditional limitations. The first one is the small number of subjects were investigated. Further, studies are needed to investigate whether our findings remain valid in a large population? The second one, in plane resolution was poor, which might be insufficient to image small lumbar spinal nerves, the low scan time (low NSA) and ADC maps were limited because the tissue contrast between nerves and surrounding tissues was poor . Therefore the b-values and ADC maps values were measured within the ROI that was placed in anatomical locations on nerves by using neurography. Third; electrophysiological examinations were not performed to detect the level of affected nerve in this study.

Conclusion

Our study demonstrated that neurography is a possible way to visualize early changes, such as nerve indentation and swelling, and to qualitatively evaluate affected lumbar nerves course in patients with lower extremity pains. We believe that, DWI has potential to be used as a tool for assessing the diagnosis of changes in affected nerve course if happened. Although not statistically significant results in all researches, our result in nerve diameter clearly showed a tendency toward decrease diffusivity in affected side (pain radiating to lower extremity) with a small swelling of the nerve tract.

Acknowledgments

References

1. Mixter WJ, Barr JS. Rupture of the Intervertebral Disc with Involvement of the Spinal Canal. N Engl J Med. 1934; 211:210-5.
2. Modic MT, Ross JS. Lumbar Degenerative Disk Disease 1. Radiology. 2007; 245(1):43-61.
3. Nachemson AL. Newest knowledge of low back pain a critical look. Clin Orthop Relat Res. 1992; 279:8-20.
4. Murai K, Sakai D, Nakamura Y, Nakai T, Igarashi T, Seo N, et al. Primary immune system responders to nucleus pulposus cells: evidence for immune response in disc herniation. Eur Cell Mater. 2010;19:13-21.
5. Shamji MF, Setton LA, Jarvis W, So S, Chen J, Jing L, et al. Proinflammatory cytokine expression profile in degenerated and herniated human intervertebral disc tissues. Arthritis Rheum. 2010;62(7):1974-82.
6. Milette PC, Fontaine S, Lepanto L, Breton G. Radiating pain to the lower extremities caused by lumbar disk rupture without spinal nerve root involvement. AJNR Am J Neuroradiol. 1995;16(8):1605-13.
7. Takata K, Takahashi K. Hamstring tightness and sciatica in young patients with disc herniation. J Bone Joint Surg Br. 1994;76(2):220-4.
8. Toyone T, Takahashi K, Kitahara H, Yamagata M, Murakami M, Moriya H. Visualisation of symptomatic nerve roots. Prospective study of contrast-enhanced MRI in patients with lumbar disc herniation. J Bone Joint Surg Br. 1993;75(4):529-33.
9. Lou ZH, Qu JR, Li HL, Liang BL, Chen JY, Wu Z, et al. Optimal technique of three-dimensional MRI of the lumbar nerve root and its radicular vein in normal and lumbar disc herniation patients. Chin Med J (Engl). 2011;124(12):1802-6.

10. Gasparotti R. New techniques in spinal imaging. Neuroradiology. 2011;53(1):195-7.

11. Zhang Z, Song L, Meng Q, Li Z, Luo B, Yang Y, et al. High-resolution diffusion-weighted MR imaging of the human lumbosacral plexus and its branches based on a steady-state free precession imaging technique at 3T. Am J Neuroradiol. 2008; 29(6):1092-4.

12. Le Bihan D, Johansen-Berg H. Diffusion MRI at 25: exploring brain tissue structure and function. Neuroimage. 2012; 61(2):324-41.

13. Ohgiya Y, Oka M, Hiwatashi A, Liu X, Kakimoto N, Westesson P-LA, et al. Diffusion tensor MR imaging of the cervical spinal cord in patients with multiple sclerosis. Eur Radiol. 2007; 17(10):2499-504.

14. Hiltunen J, Suortti T, Arvela S, Seppä M, Joensuu R, Hari R. Diffusion tensor imaging and tractography of distal peripheral nerves at 3 T. Clin neurophysiol. 2005; 116(10):2315-23.

15. Bammer R, Fazekas F. Diffusion imaging of the human spinal cord and the vertebral column. Top Magn Reson Imaging. 2003; 14(6):461-76.

16. Plank C, Koller A, Mueller-Mang C, Bammer R, Thurnher MM. Diffusion-weighted MR imaging (DWI) in the evaluation of epidural spinal lesions. Neuroradiology. 2007; 49(12):977-85.

17. Kealey SM, Aho T, Delong D, Barboriak DP, Provenzale JM, Eastwood JD. Assessment of Apparent Diffusion Coefficient in Normal and Degenerated Intervertebral Lumbar Disks: Initial Experience. Radiology. 2005; 235(2):569-74.

18. Kurunlahti M, Kerttula L, Jauhiainen J, Karppinen J, Tervonen O. Correlation of Diffusion in Lumbar Intervertebral Disks with Occlusion of Lumbar Arteries: A Study in Adult Volunteers. Radiology. 2001; 221(3):779-86.

19. Aota Y, Onari K, An HS, Yoshikawa K. Dorsal root ganglia morphologic features in patients with herniation of the nucleus pulposus: assessment using magnetic resonance myelography and clinical correlation. Spine. 2001; 26(19):2125-32.

20. Kobayashi S, Yoshizawa H, Hachiya Y, Ukai T, Morita T. Vasogenic edema induced by compression injury to the spinal nerve root: distribution of intravenously injected protein tracers and gadolinium-enhanced magnetic resonance imaging. Spine. 1993; 18(11):1410-24.

21. Beattie PF, Morgan PS, Peters D. Diffusion-weighted magnetic resonance imaging of normal and degenerative lumbar intervertebral discs: a new method to potentially quantify the physiologic effect of physical therapy intervention. J Orthop Sports Phys Ther. 2008; 38(2):42-9.

22. Eguchi Y, Ohtori S, Yamashita M, Yamauchi K, Suzuki M, Orita S, et al. Diffusion-weighted magnetic resonance imaging of symptomatic nerve root of patients with lumbar disk herniation. Neuroradiology. 2011; 53(9):633-41.